Astronomical Data Analysis Software and Systems IX
ASP Conference Series, Vol. 216, 2000
N. Manset, C. Veillet, and D. Crabtree, eds.

Deconvolution as a Tool for Improved Crowded-Field Photometry with HST

R. Butler

Mathematics & Statistics Dept., University of Edinburgh, EH9 3JZ, UK

Abstract. The conventional approach to performing crowded-field photometry, whether with ground- or space-based telescopes, is to use either PSF-fitting alone or some hybrid method of aperture photometry on neighbor-subtracted images, which also requires a PSF-fitting step. I show here that in very crowded fields, such as the cores of globular clusters, aperture photometry of sub-sampled-deconvolved HST/WFPC2 images gives statistically better results than such conventional reductions of the original data with DAOPHOT-II. Perhaps more importantly, the deconvolved images also provide the basis for improved star detection, using otherwise conventional means. The technique succeeds by exploiting the nature of the HST/WFPC2 PSF: under-sampled, spatially varying and with high-frequency structure in the wings, but yet determinable to high accuracy by sub-sampled spatially-varying modeling of first-guess Tiny Tim grids followed by empirical improvements. I develop and illustrate these conclusions using both real HST/WFPC2 data of the Milky Way bulge globular cluster NGC 6293 in the F555W and F814W bands, and realistic simulations of a globular cluster observed under similar circumstances.

1. Introduction

The nature of the HST/WFPC2 point-spread function (PSF) is such that is is (1) under-sampled by factors of 2 to 4 (Biretta et al. 1996); (2) spatially varying over the field of view (FOV) due to field-dependent aberrations etc.; and (3) characterized by considerable high-frequency structure in the "wings" ($r > (1 \rightarrow 2)\times$FWHM). As a result, residuals from determining & fitting the PSF to the image appear much larger than with well-sampled images, making it difficult to cleanly subtract stars which are "neighbors" to the PSF stars; while around bright stars, both these residuals and the high-frequency structure in the PSF wings resemble faint stars, thus causing errors in star detection (either missed detections of real objects, or false detections of "starlike" artifacts). Finally, under-sampling reduces the statistical accuracy of the fit, and fitting many thousands of overlapping star images simultaneously is a computing resources (memory & CPU) problem unless compromises are made with sub-groupings; so for these reasons some system involving aperture photometry would be more desirable, but crowding does not permit this.

2. Method and Goals

To overcome the problems outlined above when performing photometry in the dense core fields of globular clusters, a new approach was developed. The HST/WFPC2 images were pre-processed using the Maximum Entropy Method (MEM) for image deconvolution (Narayan & Nityananda 1986, Skilling & Bryan 1984). One would expect improved star detection on sub-sampled MEM - deconvolved images, because the actual complex HST PSF shape is used in the star detection process via MEM, which effectively "Gaussianises" the PSF, doubles the sampling, and better separates the stars from each other. This work also compared aperture photometry on the sub-sampled MEM-deconvolved images to the following conventional reductions of the original data: aperture photometry, profile-fitting photometry, and the hybrid method (e.g. Yanny et al. 1994) of aperture photometry on neighbor-subtracted images.

The first PSF model for each WFPC2 chip & filter combination had to be $2\times$sub-sampled, quadratically variable in a spatial sense, and a good match to the real PSF. A 6×6 grid of normal-sampled *Tiny Tim* (Krist & Hook, 1996) synthetic PSFs provided the "stars" from which *DAOPHOT-II* (Stetson 1994) computed this model PSF. But in the *STSDAS* implementation of MEM, the PSF must be spatially-invariant, so deconvolution was performed on a 6×6 grid of highly overlapping 256×256 pixel sub-images, each with its own PSF appropriate to that position on the chip. The deconvolved sub-images were then reassembled into a sub-sampled whole, upon which the star detection (using *DAOPHOT-II/DAOFIND*) and photometry steps were performed. Coaddition of deconvolved images in two bands (F555W and F814W), with a moderate rejection threshold for statistically deviant positive features, greatly suppressed deconvolution artifacts around the brighter stars[1]. Coadding also provided slightly greater depth. After a first *DAOPHOT-II/ALLSTAR* PSF-fit of the original images, a new sub-sampled, quadratically variable model was empirically computed from $\sim$90 - 100 bright stars. This second, refined PSF was then used to repeat the MEM deconvolution and PSF-fitting steps.

In addition to testing these procedures on the real HST/WFPC2 data of the Milky Way bulge globular cluster NGC 6293 in the F555W and F814W bands, other cluster images were simulated in order to quantify the photometric and astrometric performance of the technique. These are the simulated images specifications: 19957 input stars (17175 centred within the FOV); Trager et al. (1995) NGC 6293 spatial distribution (modified for a steeper form in the core); Z=0.0040, Y=0.24, Age=14 Gyr isochrone/luminosity functions of Bertelli et al. (1994); Janes & Heasley (1991) NGC 6293 apparent distance modulus (=16.0); Holtzman et al. (1995) and Whitmore (1995) HST zeropoints & photometric system calibrations; same net gain, readnoise, exposure time, saturation level, and mean background as the NGC 6293 images; $2\times$-sub-sampled, spatially varying *DAOPHOT-II* model of a *Tiny Tim* grid for input PSF with 0".015 rms pointing-jitter.

---

[1]Real stars hold steady in position, whereas deconvolution artifacts from slight PSF mismatches displace radially in the wings of stars according to the wavelength of light observed

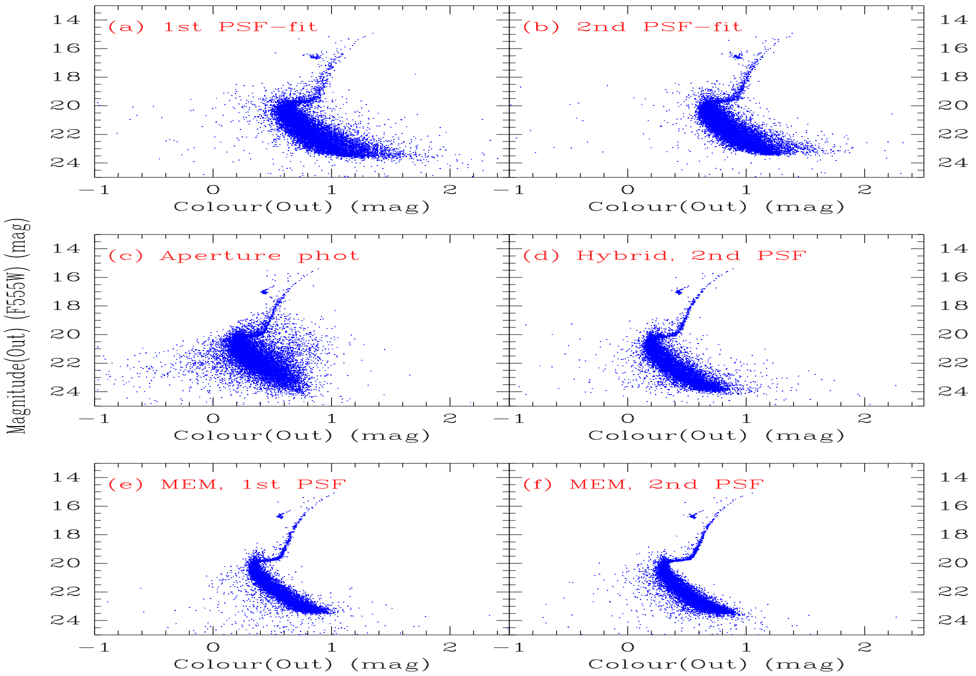

Figure 1. CMDs resulting from the six reduction techniques, for all stars in the simulated WFPC2/PC1 images.

3. Results & Conclusions

Figure 1 shows the photometric results for the simulated images and Figure 2 shows their astrometric results. Star detection rates were indeed improved: 9446 stars were found with conventional methods, but 13528 stars with MEM-preprocessing. The improvement in the photometric accuracy was more moderate. In terms of random colour deviations from the "truth" input values, aperture photometry on the subsampled MEM-deconvolved images was on a par with the hybrid method for bright objects, and somewhat better for faint objects, thus statistically better overall. NGC 6293 showed similar improvements. In Figure 2(a), 78% of all the detected stars have astrometric accuracies better than 0.1 pixels (bins 1-2); there is a power law decline due to noise (fit overplotted) from bin 3 onwards. Note the clear sub-pixel pattern in Figure 2(d): this indicates that systematic errors are induced at a level $\leq$0.1 pixel; this is fine for the purpose of crowded-field photometry, but precludes the use of this technique for high-precision astrometry. The deconvolution algorithm used should not matter, once it supports subsampling and the Poisson photon-counting and Gaussian read-out noise sources. Newer algorithms (e.g. Magain et al. (1998), which handles sampling correctly) may improve results further.

Acknowledgments. This research was supported by the TMR programme of the European Commission (contract ERBFMBICT972185). I am also grateful to my Edinburgh host, Prof. Douglas Heggie, Dr. Andy Shearer & Dr. Aaron Golden (NUI Galway, Ireland) and Dr. Alan Penny (RAL, UK) for their advice and encouragement.

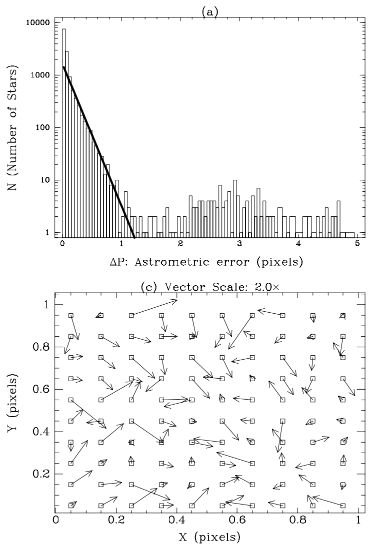

Figure 2. Astrometric analysis of the reduction of the simulated images. (a): Histogram of the ΔP $(= \sqrt{(\Delta x)^2 + (\Delta y)^2})$ errors for all stars. 1 bin = 0.05 pixel. (b): ΔP vectors with respect to distance of each star from the centre of a pixel (following Lindler et al. 1994). (c): As (b) but with vectors rebinned into 100 sub-pixel cells (on a 10×10 grid); vector magnification is 2.0× for clarity. (d): As (c) but only for stars with $\Delta P \leq 0.1$ pixel; vector magnification is 5.0×.

References

Bertelli, G., Bressan, A., Chiosi, C., Fagotto, F., & Nasi, E. 1994, A&A, 106, 275

Biretta, J. A., et al. 1996, WFPC2 Instrument Handbook, Version 4.0 (Baltimore: STScI)

Holtzman, J., et al. 1995, PASP, 107, 1065

Janes, K. A., & Heasley, J. N. 1991, AJ, 101, 2097

Krist, J., & Hook, R. 1996, Tiny Tim User's Manual, V4.2 (Baltimore: STScI)

Lindler, D., Heap, S., Holbrook, J., Malumuth, E., Norman, D., & Vener-Saavedra, P. C. 1994, in The Restoration of HST Images and Spectra II, ed. R. J. Hanisch & R. L. White (Baltimore: STScI), 286

Magain, P., Courbin, F., & Sohy, S. 1998, ApJ, 494, 472

Narayan, R., & Nityananda, R. 1986, ARA&A, 24, 127

Skilling, J., & Bryan, R. K. 1984, MNRAS, 211, 111

Stetson, P. B. 1994, PASP, 106, 250

Trager, S. C., King, I. R., & Djorgovski, S. 1995, AJ, 109, 218

Whitmore, B. 1995, in Calibrating Hubble Space Telescope: Post Servicing Mission, (Baltimore: STScI)

Yanny, B., Guhathakurta, P., Schneider, D., & Bahcall, J. 1994, ApJ, 435, L59